ORAL/POSTER REFERENCE:ICF100510PR

A VARIABLE-AMPLITUDE FATIGUE LIFE PREDICTION TAKING INTO ACCOUNT CRACK RETARDATION

Z.Perovic

Department of Mechanical Engineering, University of Montenegro,
81000 Podgorica, Yugoslavia

ABSTRACT

A bimodal concept for predicting a high-cycle fatigue life of the structural details subjected to a variable-amplitude loading is considered in this paper. The total fatigue life was separated into two phases: crack initiation and crack propagation. The portion of life spent in crack initiation was estimated by using S-N data obtained on smooth specimens. A fracture mechanics concept was used to calculate the portion of life spent in crack propagation. A modified Gray-Gallagher model was used to predict fatigue crack retardation following multiple overloads in a block spectrum. An original Gray-Gallagher model was proposed to predict fatigue crack retardation following a single overload, not taking into account either a delayed retardation or effect of multiple overloads. Both of these effects were incorporated in a modified Gray-Gallagher model used in this work. A computer program based on this model was applied to a welding joint subjected to a block spectrum loading and the results were compared with the experimental data reported in the literature.

KEY WORDS

Fatigue life prediction, crack initiation and propagation, retardation model, welded joint.

INTRODUCTION

Based on the previously determined stress distribution at the critical location, the fatigue life is calculated for each 'microelement' [Figure 1(*a*)] along the potential crack path, by using S-N data obtained on smooth specimens, as illustrated in Figure 1(b). The reciprocal derivative of this curve represents a rate of crack initiation in terms of dx/dN (x = distance from notch root; N = number of cycles), as shown in Figure 1(c). This rate may be interpreted as the rate at which the short crack grows due to the breaking of the microelements. It was proved [1] that the fatigue crack growth rate can be predicted on the basis of the smooth specimen data. A more consistent, but at the same time more complex, use of that approach would require a re-determination of the increased stress in each block when the crack tip reaches it and by taking into account the previous damage accumulation. It can be concluded that this method [1] should give a greater crack growth rate than the initiation rate obtained by the bimodal concept. However, an opposite effect is present during short crack growth, i.e. a gradual increase of crack closure level (decrease of ΔK_{eff}) which causes a decrease in crack growth rate. In this work, it is assumed, as a first approximation, that these two opposite effects are equal and so the estimated rate of crack initiation (or short crack growth) can be considered a reasonably accurate solution. The macrocrack growth rate da/dN (a = crack size; N = number of cycles) obtained by using fracture mechanics approach, is also shown in Figure 1(c). At some distance a_{i} , from the notch root, the rate of the crack initiation equals the rate of crack propagation. The upper zones of these curves, before and after this distance, indicate which of the mechanisms is more damaging. This distance a_{i}, when initiation is finished, may be regarded as the crack initiation size [2]. Determination of the crack initiation life N_{i} is based on the stress range at distance

a_i. The crack propagation life N_p is obtained by integrating the equation $da/dN = f(\Delta K)$ from a_i to a_f. The final crack size a_f can be determined from the fracture toughness of a material.

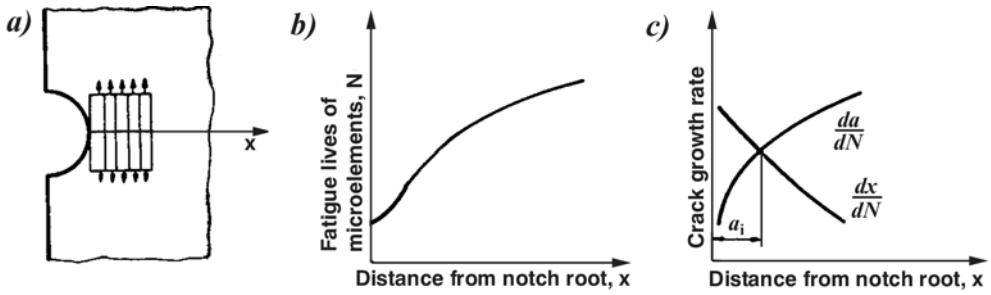

Figure 1: Schematic illustration of the bimodal concept. (*a*) Microelements; (*b*) Fatigue lives of microelements along the potential crack path. (*c*) Crack initiation and propagation rates and crack size a_i.

WELDED JOINT

The total fatigue life of non-load carrying, fillet-welded transverse stiffeners (Figure 2) subjected to spectrum loading, was determined by using the previously described bimodal concept. The specimens were welded by the automatic submerged-arc process. The mechanical properties of the steel (high-strength low-alloy structural steel, A588) plates are: σ_{ys} = 425 MPa, σ_{ts} = 569 MPa [3]. For simplicity, the influence of the microstructural heterogeneity was not considered in this paper. The S-N data, crack growth equation and relevant fracture mechanics parameters were assumed from Refs. [4-6] using average values for similar ferritic steels, i.e.
S-N curve for smooth specimens

$$log\, N = 13.785 - 3.178 log\, \Delta\sigma \tag{1}$$

The fatigue limit is $\Delta\sigma_{fls}$ = 227 MPa (stress ratio R = -1).

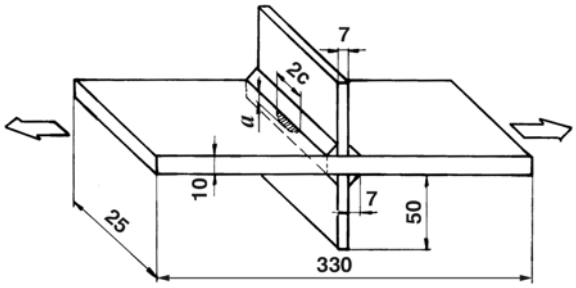

Figure 2: Welded joint; dimensions in mm.

Paris equation for the crack growth [7]

$$\frac{da}{dN} = C(\Delta K)^n \tag{2}$$

where $C = 4.8 \times 10^{-12}$, n = 3. Fracture mechanics parameters K_c = 55 MPa$\sqrt{m}$, the fracture toughness, ΔK_{th} = (3 to 8) MPa$\sqrt{m}$ (for R = 0.8÷0.1, respectively) threshold SIF range [8]. The threshold stress intensity range for various R ratios (changed by residual stress) was determined [9] by the equation:

$$\Delta K_{th} = (1 - R)^{\alpha}\, \Delta K_{th(0)} \tag{3}$$

where α is a material parameter, and $\Delta K_{th(0)} = \Delta K_{th}$, corresponding to R = 0. To get the best agreement with the experimental ΔK_{th} data [8], a value of α = 0.9 was assumed. The residual welding stresses cause a change in the R-ratio, thus influencing the fatigue strength. A typical residual welding stress pattern, through the specimen thickness along the section A-A, is shown in Figure 3(c) [curve 1]. The self-balancing stresses were assumed to vary from σ_r = 80% of the yield stress in tension at the weld toes to 40% of the yield stress in compression at the centre of the plate [10]. The load-induced elastic stress distribution in an uncracked detail, along section A-A, is given by curve 2 of Figure 3(c). To find the final stress distribution, curves 1 and 2 were superimposed, assuming identical elastic-perfectly plastic behaviour in tension and compression. Curve 3 shows the resulting

stress distribution at the top of the load cycle with the proper allowance for a redistribution of stresses in excess of yield to the adjacent elastic material. Curve 4 represents the stress distribution at the bottom of the load cycle. This curve was obtained by subtracting the elastic stress distribution, curve 2, from curve 3. If the residual stress distribution after the first cycle was unchanged, the actual stresses would cycle between curves 3 and 4. However, the mean stress relaxes during cycling; a process that is accelerated at higher stress (strain) ranges. The approximate procedure accounting for stress relaxation (described in Ref.[11]) was used in this paper.

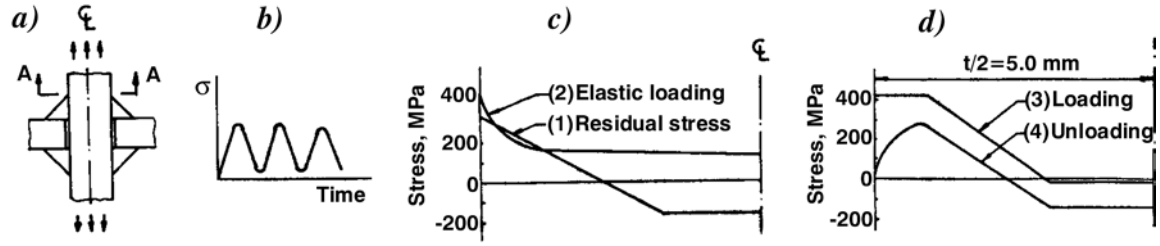

Figure 3: Superposition of residual and applied stresses

PREDICTION OF VARIABLE-AMPLITUDE FATIGUE LIVES OF A WELDED JOINT

The welded joint was subjected to block-spectrum loading (Figure 4) that simulates service loading. The normalized stress ranges ($\Delta\sigma_l/\Delta\sigma_{max}$) and the frequency of each stress level (f_l) are given in Table 1.

TABLE 1
DATA FOR BLOCK – LOADING SPECTRUM

Block number, l	1	2	3	4	5	6	7	8	9	10
Normalized stress range $\Delta\sigma_l/\Delta\sigma_{max}$	0.525	0.575	0.625	0.675	0.725	0.775	0.825	0.875	0.925	0.975
Frequency, f_l ,%	30.6	22.3	15.9	10.8	7.2	4.7	3.1	2.1	1.7	1.6

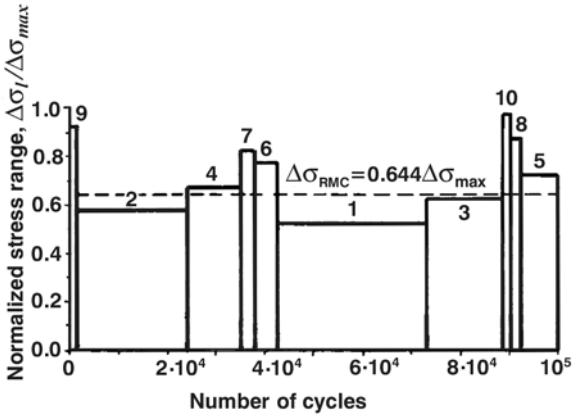

Figure 4: Block spectrum loading pattern

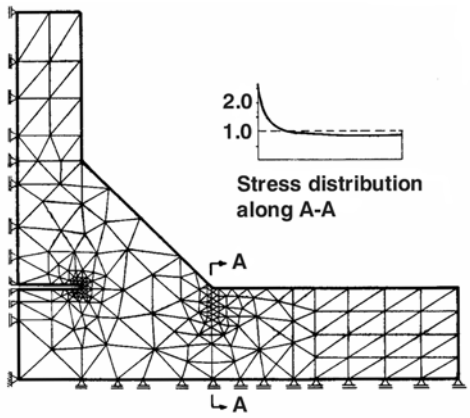

Figure 5: Finite elements mesh and stress distribution along potential crack path

The number of cycles per spectrum was 10^5 (at this block-spectrum size, the load interaction effects extend the fatigue life [12]). In order to check its reliability the bimodal concept was previously applied to the welded stiffener subjected to either constant-amplitude or spectrum loading (the spectrum size, 10^3 cycles, was chosen to avoid interaction effects as a consequence of 'delayed retardation', according to Refs [6,13]) [11]. Agreement between experimental test results and predictions was good.

Crack Initiation

The uncracked welded joint was first analysed. The stress distribution was obtained using the finite element method. Only one-quarter of the double symmetrical joint was modelled (Figure 5). A weld toe radius r = 0.5

mm (r/t = 0.05) was assumed in this work. The calculated value of the theoretical stress concentration factor is K_T = 2.6. Interaction effects, in this phase, were taken into account assuming that the residual stress relaxation during the first cycle was determined by the maximum stress range in the spectrum ($\Delta\sigma_{10}$), while the relaxation during subsequent cycling was determined by the root-mean-cube stress range ($\Delta\sigma_{RMC}$) level for the corresponding spectrum. The fatigue lives of the microelements were calculated using Miner's cumulative damage rule [14]:

$$\sum_{l=1}^{k} \frac{n_l}{N_l} = 1 \tag{4}$$

where n_l = number of cycles at stress range $\Delta\sigma_l$ in the spectrum, and N_l = number of cycles at constant stress range $\Delta\sigma_l$ that produces the failure. The fatigue life of the microelement can be obtained using Eqs. 1. and 4. to produce:

$$N = \frac{N_{10}}{\sum_{l=1}^{k} f_l \left(\frac{\Delta\sigma_l}{\Delta\sigma_{10}} \right)^{3.178}} \tag{5}$$

where N_{10} = number of cycles until failure at the highest stress range $\Delta\sigma_{10}$ in the spectrum. In these calculations Eqn. 1. was modified by Gerber's equation accounting for the effect of mean stress (changed by residual stress) on fatigue strength, i.e.

$$\Delta\sigma_{\mathrm{fs}} = \Delta\sigma_{\mathrm{fs}(0)} \left[1 - \left(\frac{\sigma_{\mathrm{m}}}{\sigma_{\mathrm{ts}}} \right)^2 \right] \tag{6}$$

where $\Delta\sigma_{\mathrm{fs}}$ = fatigue strength ($\sigma_{\mathrm{m}} \neq 0$), $\Delta\sigma_{\mathrm{fs}(0)}$ = fatigue strength ($\sigma_{\mathrm{m}} = 0$), σ_{m} = mean stress and σ_{ts} = tensile strength. Based on these values, the crack initiation rates dx/dN for the various values $\Delta\sigma_{\mathrm{RMC}}$ are calculated.

Crack Propagation

In order to take into account crack retardation following a single overload, Gray and Gallagher [15] expressed the rate of crack growth following the overload as

$$\frac{da}{dN} = C\left(\Delta K_{eff}\right)^n \tag{7}$$

where

$$\begin{aligned} \left(\Delta K_{eff}\right) &= \left(\frac{K_{max}}{K^*_{max}} \right)^{\frac{2m}{n}} \cdot \Delta K, \quad \text{if} \quad K_{max} < K^*_{max} \\ \left(\Delta K_{eff}\right) &= \Delta K, \qquad\qquad \text{if} \quad K_{max} \geq K^*_{max} \end{aligned} \tag{8}$$

K^*_{max} is given by

$$K^*_{max} = K_{max,OL} \left(1 - \frac{\Delta a}{Z_{OL}} \right)^{\frac{1}{2}} \tag{9}$$

where Δa is the crack increment since the overload and Z_{OL} is the size of the plastic zone due to the overload (load interaction zone). The shaping exponent m in Eqn. 8. was found to be:

$$m = \frac{n}{2} \left[\frac{log\left(\Delta K / \Delta K_{th}\right)}{log\left(K_{max,OL} / K_{max}\right)} \right] \tag{10}$$

An overload produces a complete crack arrest (in steel) when $S = K_{max,OL}/K_{max}$=2.3. Gray-Gallagher model predicts a sudden drop in da/dN after the overload application. However, other investigators observed that the lowest growth rate was reached after the crack had extended over approximately one eighth to one quarter of

the total overload plastic zone (this phenomenon is referred to as delayed retardation) [13]. To model the delayed retardation, it is assumed in this work, that the growth rate after an overload remains unchanged over an increment in crack length $\beta = \Delta a/Z_{OL}$. This increment decreases with increase of a number of overload cycles (for greater than 10 overload cycles, the minimum growth rate occurred almost immediately after the overload applications [16]). Because of that, it is assumed in this work that β varies from $\beta = 0.1$ for a single overload to $\beta = 0$ for greater than 10 overload cycles. The minimum value of da/dN in the load interaction zone decreases as the number of overloads increases [17]. This effect was modelled by assuming that the increase in closure level (changing ΔK_{eff}) is a function of the number of overload cycles applied [18]:

$$\gamma = \gamma_1 + (1-\gamma_1)\left(\frac{N_{OL}-1}{N_{sat}-1}\right) \tag{11}$$

where γ = ratio of the closure stress after N_{OL} overloads to the stabilized overload closure stress; γ_1 = the value of γ for $N_{OL} = 1$; N_{sat} = the number of overload cycles required to achieve saturation (that is beyond N_{sat} the addition of overload cycles produces no additional retardation). The effective stress range $\Delta\sigma_{\text{eff}}$, at lower stress level after multiple overloads, is then equal to the difference between the maximum stress, $\sigma_{\max}$, and the closure stress, σ_c:

$$\Delta\sigma_{eff} = \sigma_{max} - \sigma_c = \sigma_{max} - \sigma_{c1}\frac{\gamma}{\gamma_1} = \sigma_{max} - \left[\sigma_{max} - \left(\Delta\sigma_{eff}\right)_1\right]\frac{\gamma}{\gamma_1} \tag{12}$$

This equation can be expressed in terms of stress intensity factor:

$$\Delta K_{eff} = K_{max} - \left[K_{max} - \left(\Delta K_{eff}\right)_1\right]\frac{\gamma}{\gamma_1} \tag{13}$$

where $(\Delta K_{\text{eff}})_1$ = effective range of stress intensity factor in lower stress level following a single overload, calculated from the first of Eqs. 8. The stress intensity factor was calculated by the expression [19,20]:

$$K = F_G F \sigma \sqrt{\frac{\pi a}{Q}} \tag{14}$$

where:

$$F = \left[M_1 + M_2\left(\frac{a}{t}\right)^2 + M_3\left(\frac{a}{t}\right)^4\right] f_\varphi f_w g \;\; ; \;\; M_1 = 1.13 - 0.09\left(\frac{a}{c}\right) \; ; \; M_2 = -0.54 + \frac{0.89}{0.2 + \frac{a}{c}}$$

$$M_3 = 0.5 - \frac{1.0}{0.65 + \frac{a}{c}} + 14\left(1.0 - \frac{a}{c}\right)^{24} \; ; \; f_\varphi = \left[\left(\frac{a}{c}\right)^2 cos^2\varphi + sin^2\varphi\right]^{\frac{1}{4}} \; ; \; f_w = \left[sec\left(\frac{\pi c}{2w}\sqrt{\frac{a}{t}}\right)\right]^{\frac{1}{2}}$$

$$g = 1 + \left[0.1 + 0.35\left(\frac{a}{t}\right)^2\right](1 - sin\varphi)^2 \; ; \; Q = 1 + 1.464\left(\frac{a}{c}\right)^{1.65},$$

where c = major semi-axis of the elliptical crack; t,w = thickness and width of the main plate of a welded joint, respectively; φ = angle that describes the location at the crack front with respect to the major axis of the ellipse. The values of the crack axis ratio a/c were assumed from Ref. [5]. The geometry correction factor is

$$F_G = \frac{2}{\pi}\sum_{i=1}^{n}\frac{\sigma_{bi}}{\sigma}\left(arcsin\frac{b_{i+1}}{a} - arcsin\frac{b_i}{a}\right) \tag{15}$$

where σ_{bi} is the normal stress in a finite element between the distance b_{i} and $b_{\text{i+1}}$. This accounts for the effect on K of a stress concentration produced by a structural detail. Verreman *et al.* [21] used this method for determination of F_{G} factor of a cruciform-welded joint and compared it with the accurate solution obtained by using high-order crack tip elements with an inverse square root singularity. They reported differences smaller than 6%, so this method can be considered accurate for engineering purposes. The advantage of Albrecht's

method is that only one stress analysis needs to be made for each joint geometry, i.e. the stress analysis of an uncracked joint. The values of γ_1 and N_{sat} (γ_1 = 0.70; N_{sat} =500) were selected to provide the best fit of the predicted crack propagation life to the experimental data for the welded stiffeners (of the same material) with known initial cracks [5]. The crack propagation rate was calculated using Eqn. 7.

Total Fatigue Life

The crack initiation size a_i is determined by using the crack initiation rate curve and the crack propagation rate curve. The crack initiation life N_i is determined using Eqn. 5. with the stress range for the distance a_i. The crack propagation life N_p is calculated by solving Eqn.7. from a_i to a_f by the Runge-Kutta method (using the computer program). The total fatigue life is obtained by summing the initiation and propagation lives. The predicted fatigue lives for various equivalent stress ranges ($\Delta\sigma_{RMC}$ = 133; 196; 249 MPa) as well as experimental data [12] are shown in Figure 6.

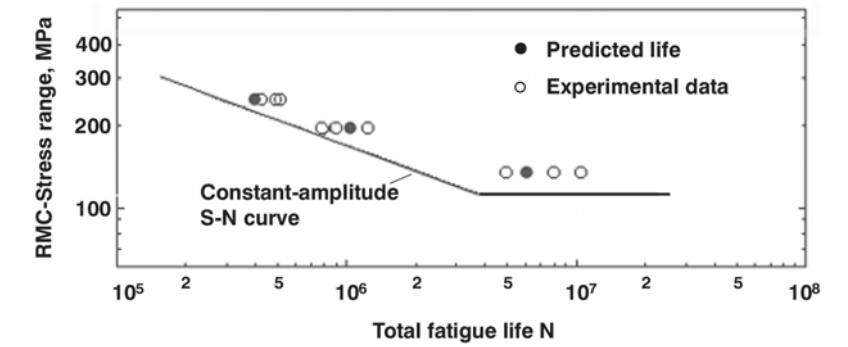

Figure 6: Comparison of predicted fatigue lives with experimental data

REFERENCES

1. Glinka, G. (1985) *Eng. Fract. Mech.* 21, 245.
2. Socie, D.F. Morrow, J. and Chen, W.C. (1979) *Eng. Fract. Mech.* 11, 851.
3. Albrecht, P. and Friedland, M. (1979) *J. Struct. Division, ASCE* 105(12), 2657.
4. Albrecht, P. and Rubeiz, C.G. (1987) *Variable Amplitude Load Fatigue.*Report No. DTFH61-86-C-0036-II, University of Maryland.
5. Albrecht, P. and Sahli, A. (1984) In: *Fracture Mechanics,*ASTM STP 833, pp.193-217, Sanford, R.J. (Ed).
6. Abtahi, A., Albrecht, P. and Irwin, G.R. (1977) In: *Mechanics in Engineering,* University of Waterloo Press, pp.313-334.
7. Paris, P.C. and Erdogan, F. (1963) *Trans. ASME, J. Basic Eng.,* 85(4), 528.
8. Paris, P.C., Bucci, R.J., Wessel, E.T., Clark, W.G. and Mager, T.R. (1972) ASTM STP 513, pp. 141-176.
9. Klesnil, M. and Lukas, P. (1972) *Mater. Sci. Eng.* 9, 231.
10. Abtahi, A., Albrecht, P. and Irwin, G.R. (1976) *J. Struct. Division,* ASCE 102(11), 2103.
11. Perovic, Z. (1998) *Fatigue Fract. Eng. Mater. Struct.* 21, 1559.
12. Albrecht, P. and Yamada, K. (1979) In: *Service Fatigue Loads Monitoring, Simulation and Analysis,* ASTM STP 671, pp. 255-277, Abelkis, P.R. and Potter, J.M. (Eds).
13. Von Euw, E.F.J., Hertzberg, R.W. and Roberts, R. (1972) In: *Stress Analysis and Growth of Cracks,* ASTM STP 513, pp. 230-259.
14. Miner, M.A. (1945) *J. Appl. Mech.* 12, *Trans.ASME,* 67, A-159.
15. Gray, T.D. and Gallagher, J.P. (1976) In: *Mechanics of Crack Growth,* ASTM STP 590, pp. 331-344.
16. Corbly, D.M. and Packman, P.F. (1973) *Eng. Fract. Mech.* 5, 479.
17. Trebules, V.W., Roberts, R. and Hertzberg, R.W. (1973) In: *Progress in Flaw Growth and Fracture Toughness Testing,* ASTM STP 536, pp. 115-146.
18. Bell, P.D. and Wolfman, A. (1976) In: *Fatigue Crack Growth Under Spectrum Loads,* ASTM STP 595, pp. 157-171, Wheeler, J. B. (Ed).
19. Newman, J.C. and Raju, I.S. (1984). NASA TM 85793, NASA Langley Research Center, Hampton, USA.
20. Albrecht, P. and Yamada, K. (1977) *J. Struct. Divis.,* ASCE 103(2), 377.
21. Verreman, Y., Bailon, J.P. and Masounave J. (1987) *Fatigue Fract. Eng. Mater. Struct.* 10(1), 17.